Cylindrical resonator antenna manufactured with Barium Neodymium Titanate

I. NICOLAESCU[a]*, O. G. AVĂDANEI[b], S.-B. BALMUŞ[c]
[a]*Military Technical Academy, Communications and Military Electronic Systems Department, Bucharest, Romania*
[b]*Alexandru Ioan Cuza University, Iasi*
[c]*Gheorghe Asachi University*

The rapid evolution of GPS, mobile and wireless communication systems in the last years is based, substantially, on ceramic based dielectrics with effect on miniaturization of components (antennas, filters, oscillators), cost and temperature stability. The development of high dielectric constant materials was critical for the dimensions reduction of the equipment but also for their performance improvements. These materials have high dielectric constant, ε_r, between 20 and 90 ; low losses in microwave and millimetre wave domain and a low variation of dielectric constant with the temperature. The paper describes a high dielectric constant material, Barium Neodymium Titanate - $(Ba,Pb)Nd_2Ti_5O_{14}$ (BNT), and presents some results obtained by using this ceramic based material to manufacture a dielectric resonator antenna.

1. Introduction

Special materials play an increasingly more important role in electronic engineering. They are used either to manufacture active and passive devices or to modify the parameters of such devices. An important trend in electronic engineering and telecommunications is the miniaturization of electronic components. In the microwave range this can be done by increasing the dielectric permittivity of the materials the passive components are made of. High dielectric permittivity materials are very difficult to manufacture. Usually a very complex technological process is needed [1, 2]. In addition to high complexity very high temperatures are used during processing the materials. This paper presents some results of simulations and measurements obtained with a dielectric resonator antenna manufactured with $(Ba,Pb)Nd_2Ti_5O_{14}$ - Barium Neodymium Titanate (BNT) .

2. Barium Neodymium Titanate (BNT)

The unmodified barium titanate exhibit very high dielectric constant but also high dielectric loss around room temperature because its ferroelectric state. In order to decrease the microwave losses of a bulk ferroelectric material, it has to be in the paraelectric phase [2].

Such ternary oxide dielectric compounds as BaO-TiO_2-Ln_2O_3 , where Ln is a lanthanide, but most of the time Ln = Nd, Sm, are very attractive for microwave applications due to the high dielectric permittivity and moderate low loss. In this paper the case Ln = Nd is investigated. The variation of the dielectric constant versus temperature showed a significant decrease of the Curie temperature with Nd content [3].

As it was previously shown, due to the high polarizability of the lead ion, addition of the PbO to the barium neodymium titanate, increases the values of the microwave dielectric constant [4]. At the same time, the increase of Pb content decreases slightly the product between the quality factor Q ($Q = 1$ / tan δ) and the measurement frequency f. Moreover, in the case of the addition of a half a mole of lead oxide, the temperature coefficient τ_f of the resonance frequency takes negative values, while for the barium neodymium titanate without Pb, τ_f is positive [5].

For $(Ba,Pb)Nd_2Ti_5O_{14}$ preparation, barium carbonate and Ti, Nd oxides were used as raw materials. The lead oxides was added substitutional for barium oxide. Small amount (less than 0.2 wt %) of nikel oxide and zinc oxide are added in order to improve the sintering process and to achieve higher bulk density. When the sintering temperature was varied between 1230 $^{\circ}$C to 1260 $^{\circ}$C, the Q x f product does not vary significantly, but a slight increase in dielectric constant was noticed due to the better densification of the material [5].

The BNT dielectric resonators were characterized in microwaves by investigating the resonances of a cylindrical BNT resonator sandwiched between two conductive planes. The resonator was magnetically coupled to an E8361A network analyzer from Agilent [6]. The measured frequency for the TE_{011} mode was 2.532 GHz [6].

Due to high dielectric permittivity, if the losses can be controlled by doping, these materials can be used in other applications, too [7, 8].

3. Cylindrical resonator antenna with BNT

A cylindrical resonator antenna, with diameter Ø = 16,6 mm, and height h = 9,7 mm is considered. It is manufactured from BNT N5-R3 material, with $\varepsilon_r = 82,7$ and tan δ=5.2 10^{-4}.

There are several possibilities to feed the dielectric resonator antennas. The feeding system depends on the shape of the resonator, the operational frequency and the dominant mode one wants to excite within the resonator. The first option is to use a probe for feeding the antenna. According to probe position the $TM_{01\delta}$ mode or $HE_{11\delta}$ can be excited within the resonator [3,9]. Another way of feeding dielectric resonator antenna is by aperture coupling. In this case the resonator antenna is placed over a conductive surface which has a rectangular slot. The coupling coefficient depends of the dimension of the slot. This method of feeding is also important because it provides a unidirectional antenna pattern, reducing the spilling radiation beneath the ground plane. From coupling point of view the slot is equivalent with a magnetic current directed along the aperture. So, in order to excite a certain mode the slot should be placed in a position where the magnetic field has to be maximum. The dimensions of the slot antenna are computed as a function of frequency and such as the area of the aperture to be minimized in order to decrease the side lobes levels below the ground plane. The length of the slot has to be chosen such as the coupling coefficient with the feeding line to be high enough but, on the same time, to avoid resonances within the operational frequency band. According to [9] the length of the solt l_s is given by the formula:

$$l_s = \frac{0,4\lambda_0}{\sqrt{\varepsilon_r}} \qquad (1)$$

where

$$\varepsilon_e = \frac{\varepsilon_r + \varepsilon_s}{2} \qquad (2)$$

and ε_r, ε_s are the resonator and substrate dielectric relative permittivity.

The width of the slot has to be as narrow as possible (0.2 l_s). It is fed using either a microstrip line or a coaxial cable. When using a microstrip line the distance between the end of the line and the slot has to be a quarter of the microstrip wavelength.

The cylindrical resonator antenna is fixed on an alumina substrate 60 mm by 48 mm by 0.5 mm. It has a metallic surface on side and the feeding microstrip line on the other side. The dielectric permittivity of the alumina is $\varepsilon_{rAl} = 9,6$. In order to feed the antenna a slot, 6 mm long and 1 mm wide, is cut into the ground plane. The centre of the slot is placed at x=0, y=5 mm coordinates. The slot is fed using a microstrip line 0.5 mm wide. The layout of the antenna is pictured on Fig. 1.
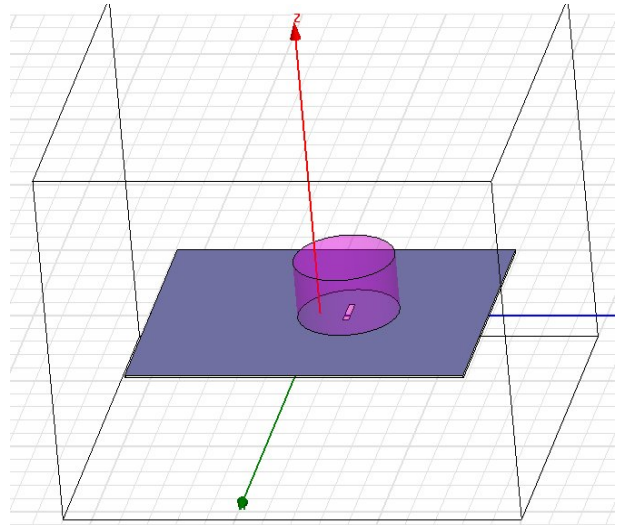

Fig. 1 Cylindrical resonator antenna fed by a slot coupled microstrip line.

For simulations we used the HFSS 11.1 software and the dimensions of the radiation box were: 70 mm, along the x axis, 80 mm, along y, and 60 mm along z axis is considered. The excitation of the entire structure was made by a lumped port. The coupling between microstrip line and resonator depend on the slot dimensions and microstrip line length. For the beginning a microstrip line length of 40 mm has been chosen.

The electromagnetic problem was solved at 6 GHz, and the convergence target was a delta S bellow 1%, for two successive iterations. Convergence was obtained after 12 iterations, and for 56670 tetrahedrons. The mesh structure is presented on Fig. 2.
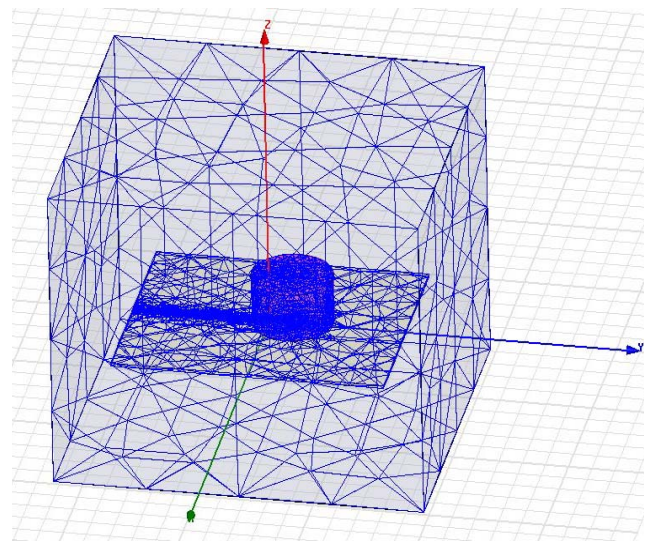

Fig. 2 Mesh plot

The first parameter which has been analysed was the return loss. It is pictured on Fig. 3. The resonator exhibits 8 resonance frequencies with different values of S_{11}, from -1.4 dB to -16.24 dB. Although the pattern simulations have been made for all resonance frequencies only the results for m4, m5 and m6 (Fig. 3) are presented below.
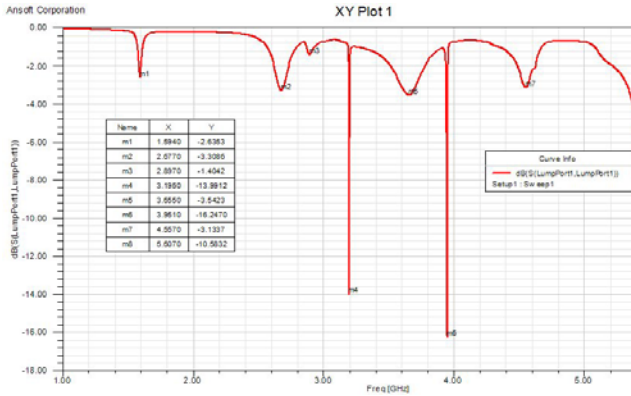

Fig. 3 The return loss for a cylindrical DRA coupled to a 40 mm microstrip line with a 6 mm by 1 mm slot.

The radiation pattern for 1.594GHz is presented in figure 4. It can be seen that the parameters of the pattern are quite constant as phi angle varies from 0^0 to 90^0.
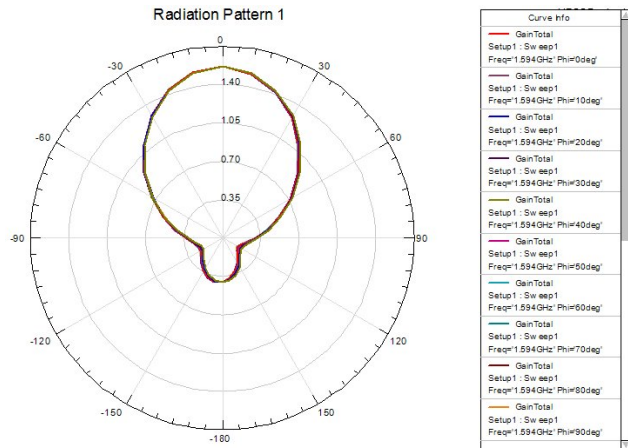
Fig. 4. Radiation pattern of the DRA fed by a slot 6mm, on 1mm, from a 40 mm length microstrip at 1.594GHz

The radiation patterns for the following modes are presented in figures.

For the 3.195 GHz resonance the gain of the antenna is pretty low, this mode having a poor impedance matching but also very low radiation efficiency.
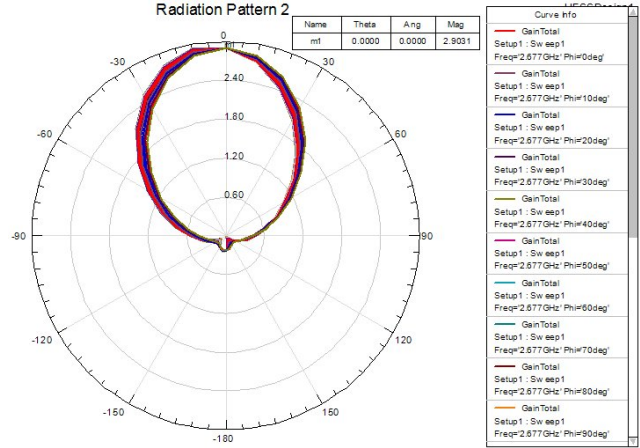

Fig. 5. Radiation pattern of the DRA fed by a slot 6mm, on 1mm, from a 40 mm length microstrip at 2.677GHz
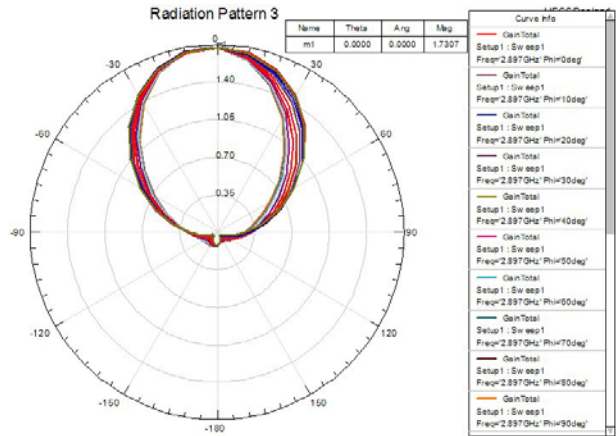

Fig. 6. Radiation pattern of the DRA fed by a slot 6mm, on 1mm, from a 40 mm length microstrip at 2.897GHz
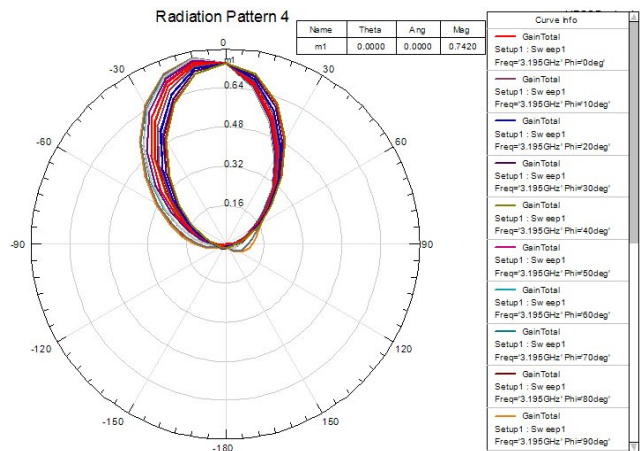

Fig.7. Radiation pattern of the DRA fed by a slot 6mm, on 1mm, from a 40 mm length microstrip at 3.195GHz

The next radiation mode analysed was for 3.655GHz. The radiation patterns for different values of phi angle are displayed on Fig. 7. The maximum value of the antenna gain is 3.79 dB. Even with a low impedance match this mode has the greatest radiation efficiency. The excitation structure was chosen to assure the excitation of as many modes as possible, not to achieve the best impedance match for only one mode, and a good impedance for all the modes is impossible.
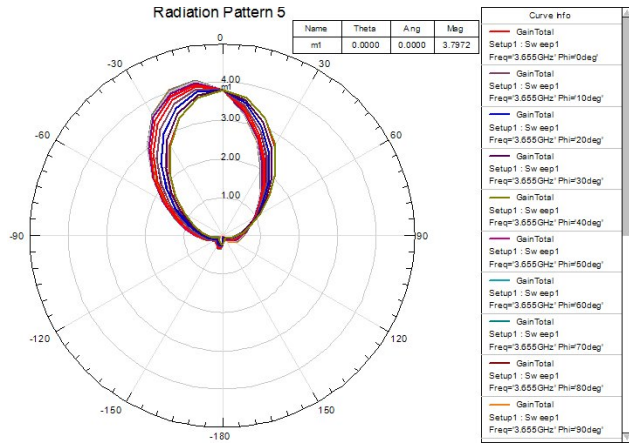
resonance frequencies can be identified with different values of return loss from -1.41 dB (2.95 GHz) to -28.80 dB (4.34 GHz). A different microstrip length would lead to a different impedance match, but also to a frequency shift of the modes. With a 48 mm length microstrip line the impedance match was better for the first and fifth resonance but worst for the second and fourth. In conclusion changing the microstrip line length we can improve the impedance match for some modes but not for all.

Fig. 8. Radiation pattern of the DRA fed by a slot 6mm, on 1mm, from a 40 mm length microstrip at 3,655GHz

Fig. 10 The simulated return loss for the DRA coupled to a 48mm microstrip line by a 7mm on 2mm slot.

The radiation patterns for 3,951 GHz are pictured on figure 9. Unlike the previous patterns in this case the shape of the pattern is much more dependent on the value of the phi angle. In addition the maximum value of the antenna gain is very low, 0.099 dB, which means that, for this frequency, the energy is not transmitted outside the antenna system.
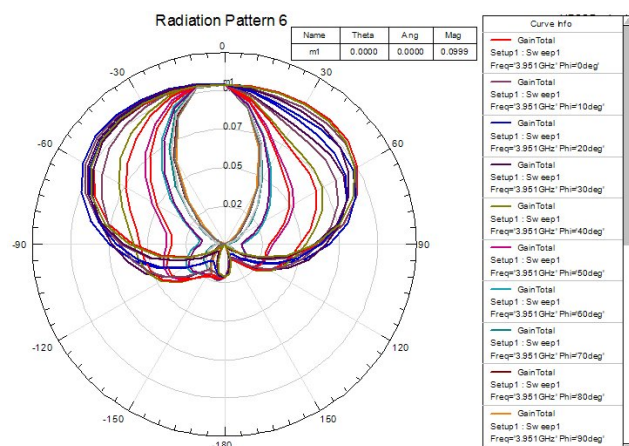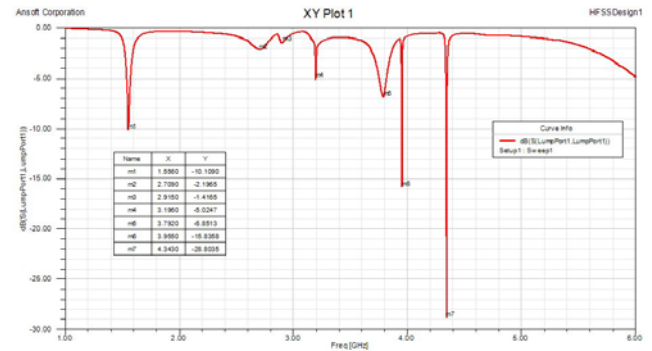
The radiation patterns for 3.79 GHz are presented on next picture. It is not perfectly symmetrical but the shape is quite stable with phi angle and the maximum gain is around 4. Comparing figures 8 and 11 we can see that this is the same mode but the resonant frequency has shifted from 3,655GHz to 3.792 GHz.
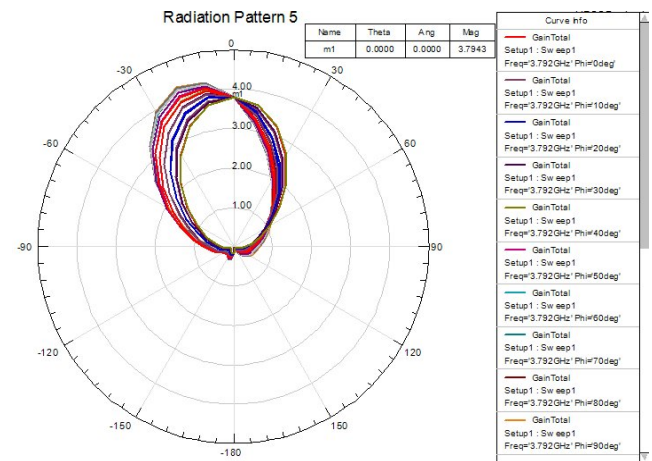

Fig. 9. Radiation pattern of the DRA fed by a slot 6mm, on 1mm, from a 40 mm length microstrip at 3,951 GHz

Fig.11. Radiation pattern for DRA coupled to a 48 mm microstrip line by a 7 mm on 2 mm slot at 3,792GHz

Other simulations have been made by feeding the dielectric resonator antenna with a 7 mm by 2 mm slot cut in the ground plane at x=0 and y=6 mm. The magnitude of S_{11} is pictured on Fig. 7. As in the previous case several

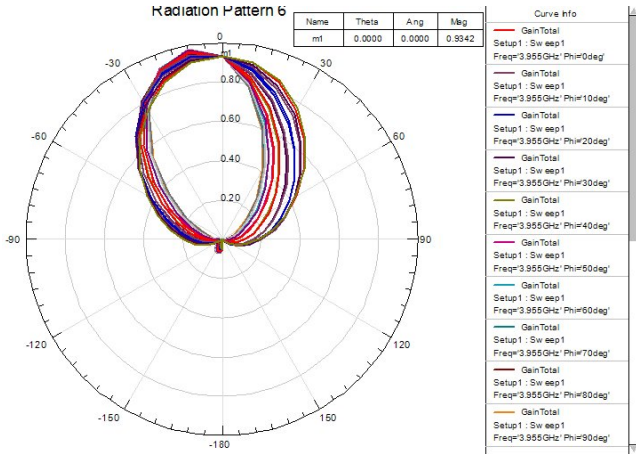In Fig. 9 the radiation patterns for 3.955 GHz are displayed.

Fig. 12. Radiation pattern for DRA coupled to a 48 mm microstrip line by a 7mm on 2mm slot at 3,955GHz

Comparing the radiation pattern from figures 9 and 12 we can see that they belong to different modes. In conclusion for a different microstrip line some mode can no longer be excited, and others can appear.

4. Experimental results

In order to check the simulations, the voltage standing wave ratio (VSWR) for a dielectric resonator antenna coupled to a 48 mm microstrip line by a 7 mm on 2 mm slot has been measured. The results are pictured on figure 13.
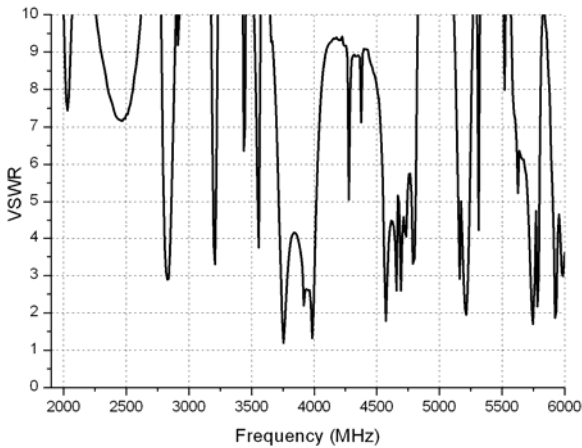

Fig. 13 The measured voltage standing wave ratio (VSWR) for the DRA coupled to a 48 mm microstrip line by a 7mm on 2mm slot

The measurements results did not fit very well the results obtained in simulations, and the only parameter that could be different in reality from simulation was the position of the resonator above the ground plane. Until now we considered that the distance between the resonator and the ground plane is 0. However in reality there is an air gap between them. In figures 14-16 we present the simulated return loss for the DRA coupled to a 48mm microstrip line by a 7mm on 2mm slot and with an air gap of 10, 30 and 50μm.
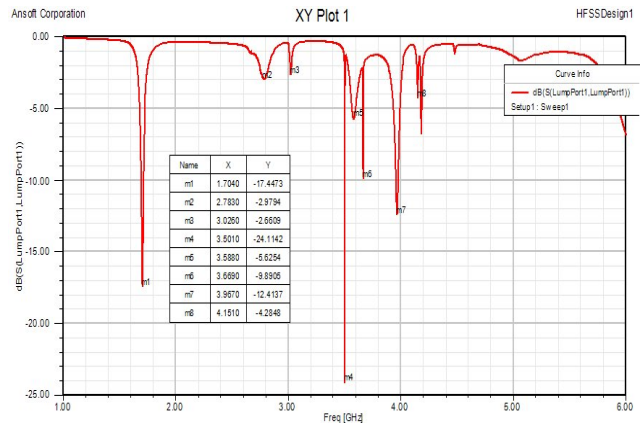

Fig. 14 The simulated return loss for the DRA coupled to a 48mm microstrip line by a 7mm on 2mm slot and with an air gap of S_{11} 10μm

From these figures we can see a considerable influence of the air gap thickness. From measurements we estimate that the air and glue thickness was around 50μm and for this thickness we obtained the best fit between measurements and simulations.
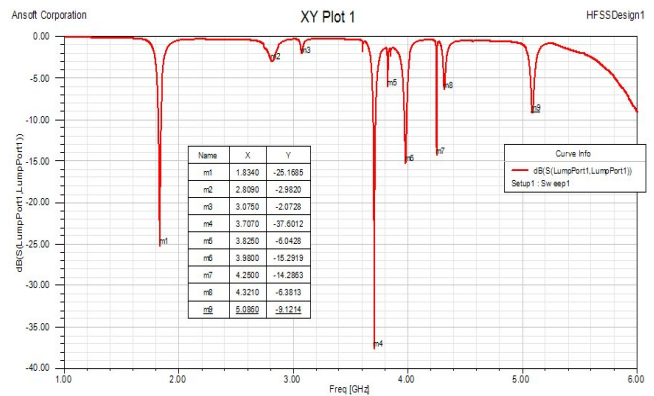

Fig. 15 The simulated return loss for the DRA coupled to a 48mm microstrip line by a 7mm on 2mm slot and with an air gap of S_{11} 30μm.
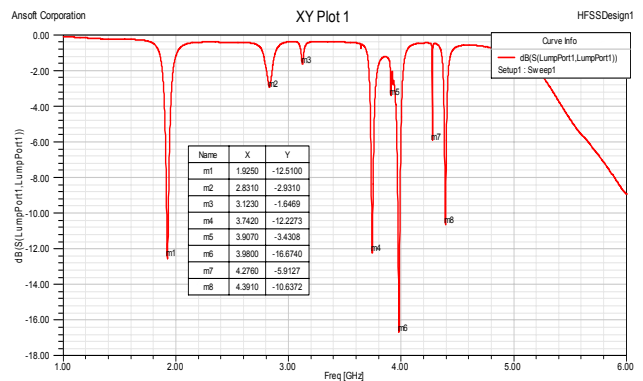

Fig. 16 The simulated return loss for the DRA coupled to a 48mm microstrip line by a 7mm on 2mm slot and with an air gap of S_{11} 50μm [6]

In measurements the first resonance appears at 2.028 GHz, and in HFSS simulations with an air gap of 50 µm the first resonance is at 1.925GHz. The second resonance has a 2.829 GHz frequency in measurements and 2.831GHz in simulations. The third resonance in measurements was at 3.205 GHz, and 3.123 GHz in simulations. The deepest S_{11} resonance obtained in measurements appeared at 3.754 GHz and had -21.27 dB magnitude. In HFSS simulation, a -12.22 dB return loss resonance at 3.742GHz was obtained. Another return loss resonance was obtained in measurements at 3.916 GHz and at 3.907GHz in HFSS. The next resonance was spotted at 3.983 GHz in measurements and there is a 3.98 GHz resonance in HFSS simulation. As we can see, with an air gap of 50µm, there is a very good concordance between measurements and simulations. The compactness and the possibility of feeding with a microstrip line recommend this antenna for null steering arrays [11].

5. Conclusions

The Barium Neodymium Titanate (BNT) material exhibits pretty high dielectric permittivity, high temperature stability and was used for a dielectric resonator antenna.

The antenna was fed using a microstrip line with different dimensions and there were several resonance frequencies for each case. The resonance frequencies are influenced by the length of the feeding microstrip line and by the dimension of the slot. The dielectric resonator antenna has a resonance at 3.655 GHz when is fed with 40 mm length microtrip line and 6 mm X 1mm slot and 3.79 GHz when the microstrip line is 48 mm long (7 mmX2 mm slot). The antenna gain for the two cases is 3.79 and approximately 4 dB. For the other frequencies the gain of the antenna is quite low.

The excitation of different modes depends on the microstrip length, slot dimensions and air gap between resonator and ground plane.

In regards to the values of the resonance frequencies, the measured return loss data show a good agreement with the simulations. However, there are some differences between the simulated and measured values of the return loss.

References

[1] A. Ioachim, M. I. Toacsan, M. G. Banciu, L. Nedelcu, G. Stoica, G. Annino, M. Cassettari, M. Martinelli, R. Ramer, J. Optoelectron. Adv. Mater., **5**(5),1395 (2003).
[2] A. Ioachim, H. V. Alexandru, C. Berbecaru, S. Antohe, F. Stanculescu, M. G. Banciu, M. I. Toacsan, L. Nedelcu, D. Ghetu, A. Dutu, G. Stoica, Mater. Sci. Eng. C **26**, 1157 (2006).
[3] I. Nicolaescu, A. Ioachim, I. Toacsan, I. Radu , G. Banciu, J. Optoelectron. Adv. Mater. **9**(11), 3592 (2007).
[4] A. Ioachim, M. I. Toacsan, M. G. Banciu, L. Nedelcu, H. Alexandru, C. Berbecaru, D. Ghetu, G. Stoica, Mater. Sci. Eng. B **109,** 183-187 (2004).
[5] A. Ioachim, M. I. Toacsan, M. G. Banciu, L. Nedelcu, C.A. Dutu, G. Stoica, J. Optoelectron. Adv. Mater. **9**(5), 1572 (2007).
[6] O. G. Avadanei, M. G. Banciu, I. Nicolaescu, L. Nedelcu, IEEE Trans. Antennas Propag. **60** (11), 5032-5038 (2012).
[7] I. Nicolaescu, J. Optoelectron. Adv. Mater. **8**(1), 333 (2006)
[8] I. Nicolaescu, J. Optoelectron. Adv. Mater. **11**(5), 728 (2009).
[9] I. Nicolaescu, A. Radu, A. Ioachim, C. Vizitiu, J. Optoelectron. Adv. Mater. **2**, 267 (2010).
[10] A. Petosa, Dielectric Resonator Antenna Handbook, Artech House, Inc. USA, 2007.
[11] I. Nicolaescu, F. D. Losif; 5th International Conference on Telecommunications in Modern Satellite, Cable and Broadcasting Service (TELSIKS 2001) 2, 679 (2001).

_____

[*]Corresponding author: ioan_nic@yahoo.com